MECSOL Joinville 2017

April 26-28, 2017
Joinville, Santa Catarina, Brazil

A LOWER BOUND LIMIT ANALYSIS OF REISSNER-MINDLIN PLATES BY FINITE ELEMENT AND SECOND-ORDER CONE PROGRAMMING

E.L.B. Cavalcante[1]*, E. Lucena Neto[1]

[1]Instituto Tecnológico de Aeronáutica, 12228-900, São José dos Campos, SP, Brazil

*Corresponding author: ericlb@ita.br

Abstract: A three-node triangular finite element is formulated for the static theorem of limit analysis to discretize Reissner-Mindlin plates. The element satisfies the equilibrium equations and the mechanical boundary conditions in a weak sense, but satisfies rigorously the von Mises yield criterion in the bending moment and shear force space. The stated nonlinear convex optimization problems are cast as second-order cone programming and solved with the MOSEK interior-point optimizer. Benchmark examples illustrate that the convergence of the results with the proposed element may not be monotonic, or even from below, but very accurate results are soon reached.

Keywords: Reissner-Mindlin plates, lower bound, finite element, second-order cone programming

6th International Symposium on Solid Mechanics

Click on the box to select the Mini-Symposia:

☐ Multiaxial and Fretting Fatigue (*Edgar Mamiya* and *Lucival Malcher*);

☐ Composite Materials (*Ricardo de Medeiros*);

☐ Constitutive Models I – Plasticity and Damage (*Lucival Malcher*, *Miguel Vaz Jr.* and *Edgar Mamiya*);

☐ Constitutive Models II – Viscoelastic and Viscoplastic Solids: Models and Applications (*Heraldo Mattos*);

☐ Impact Engineering (*Marcílio Alves*);

☐ Structural Reliability Methods and Reliability-Based Design Optimization (*André Beck*);

☐ Topology Optimization of Multifunctional Materials, Fluids and Structures (*Eduardo Lenz Cardoso* e *Emilio Carlos Nelli Silva*);

☐ Topological Derivatives: Theory and Applications (*André Novotny*);

☐ X-FEM, G-FEM and Meshfree Methods (*Roberto Dalledone Machado* and *Rodrigo Rossi*);

☐ High Order Finite Elements (*Marco Lúcio Bittencourt*);

☒ Nonlinear Analyses (*Eduardo Campello*);

☐ Other section;

MECSOL Joinville 2017

April 26-28, 2017
Joinville, Santa Catarina, Brazil

A Lower Bound Limit Analysis of Reissner-Mindlin Plates by Finite Element and Second-order Cone Programming

Eric L. B. Cavalcante
Instituto Tecnológico de Aeronáutica
ericlb@ita.br

Eliseu Lucena Neto
Instituto Tecnológico de Aeronáutica
eliseu@ita.br

ABSTRACT

A three-node triangular finite element is formulated for the static theorem of limit analysis to discretize Reissner-Mindlin plates. The element satisfies the equilibrium equations and the mechanical boundary conditions in a weak sense, but satisfies rigorously the von Mises yield criterion in the bending moment and shear force space. The stated nonlinear convex optimization problems are cast as second-order cone programming and solved with the MOSEK interior-point optimizer. Benchmark examples illustrate that the convergence of the results with the proposed element may not be monotonic, or even from below, but very accurate results are soon reached.

Keywords: Reissner-Mindlin plates, lower bound, finite element, second-order cone programming

1 INTRODUCTION

In the design of structures, the maximum load to be resisted at the impending collapse must be evaluated. The ability of the methods to accurately estimate ultimate limit states depends on the fulfillment of theoretical requirements derived from continuum mechanics concerning the equilibrium, strain-displacement relations, constitutive behavior and boundary conditions. Under certain conditions, the theory of plasticity allows lower and upper bound predictions of the collapse load by means of the static and kinematic theorems, respectively [1]. Coupling these theorems with the finite element method, as originally proposed by Hayes and Marçal [2], Hodge and Belytschko [3] and Lysmer [4], gives rise to large-scale constrained optimization problems which can be solved by means of mathematical programming.

The usefulness of this very powerful procedure was limited initially by the lack of robustness of the algorithms that were available for solving large-scale problems and by the low computational capability. Considerable challenge has been posed and significant progress has been made over the years [5-14]. Now, efficient predictions of the collapse load can be made and the procedure has become a simpler alternative to elastoplastic finite element approaches, which require the

computationally expensive effort of an evolutive analysis that follows the whole history of loading [15].

Part of these substantial advances, which has played a key role in the recent progress of limit analysis of plate structures [16-26], is related to solving large-scale nonlinear convex optimization problems [10-14]. The static approach of limit analysis was employed in [19, 20, 25]. Le *et al.* [19] utilized an adaptive element-free Galerkin method based on the Kirchhoff plate assumption. Le *et al.* [20] also considered Kirchhoff plates with an enhanced Morley element based on a second-degree moment field. Bleyer and de Buhan [25] employed semi-continuous generalized stress fields with quadratic interpolation of moments and linear interpolation of shear forces. Their formulation is addressed to Reissner-Mindlin plates.

Little work has been devoted to thick plates. The work of Cecchi *et al.* [16] on masonry walls, for instance, considered a Reissner-Mindlin kinematic limit analysis finite element, in which dissipation is produced at the elements edges due to bending moment, torsion, and shear. In [21], quadrilateral finite elements have been proposed to solve the kinematic approach for thick plates adopting a mixed B-bar strain formulation to alleviate shear locking. More recently, shear locking is also alleviated by Le [24] approximating the displacement fields of a three-node triangular finite element using the discrete shear gap method in combination with an edge-based strain smoothing technique, while Nguyen-Thoi *et al.* [26] employed a cell-based strain smoothing technique.

To the authors' knowledge the only finite element formulation developed so far for the lower bound limit analysis of thick plates seems the one by Bleyer and de Buhan [25]. Since the moments are not interpolated linearly but quadratically, the adopted von Mises yield criterion is not satisfied pointwisely over the element in [25].

We propose herein a three-node triangular finite element for the lower bound limit analysis of Reissner-Mindlin plates. The element, which has its roots in the classic paper by Anderheggen and Knöpfel [27], satisfies the equilibrium equations and the mechanical boundary conditions on average and nowhere their generalized stress fields violate the adopted von Mises yield criterion. The formulation of the static theorem is then written within the framework of a nonlinear convex optimization technique, known as second-order cone programming (SOCP) [28]. Although a solution obtained with this equilibrium model is not a strict lower bound, very accurate results are reached.

There is no analytical approach for the solution of general convex optimization problems, but there are very effective methods for solving them [29]. The interior-point method employed in this paper works extremely well in practice. It was developed by Andersen *et al.* [13] and implemented in the solver MOSEK to address nonlinear convex optimization problems, such as second-order cone programs. Predictions of the collapse load for some well-known plate problems are computed after the discrete problem is formulated as SOCP. Results are compared with exact or approximate solutions available in the literature.

2 STATIC THEOREM

The limit analysis relies on the assumption of an elastic-perfectly plastic material with a flow rule associated to a convex yield surface, and also on small displacement gradients so that the solid does not undergo large deformation at collapse. The lower bound approach follows the static theorem, which requires that the assumed stress field must satisfy the equilibrium equations, the mechanical

boundary conditions and the yield criterion everywhere. Under these idealized conditions, the computed limit load is a lower bound on the true collapse load [30].

2.1 Equilibrium Equations

Let Ω be the region occupied by the midsurface of a Reissner-Mindlin plate subjected to a distributed transverse load q. With the convention shown in Figure 1a, the plate bending is described by the equilibrium equations

$$\boldsymbol{DM} - \boldsymbol{Q} = \boldsymbol{0} \qquad \boldsymbol{\nabla}^T \boldsymbol{Q} + q = 0 \tag{1}$$

where $\boldsymbol{M} = \lfloor M_x \quad M_y \quad M_{xy} \rfloor^T$ collects the bending moments M_x, M_y and the twisting moment M_{xy}, and $\boldsymbol{Q} = \lfloor Q_x \quad Q_y \rfloor^T$ collects the shear forces Q_x, Q_y. The differential operators

$$\boldsymbol{D} = \begin{bmatrix} \dfrac{\partial}{\partial x} & 0 & \dfrac{\partial}{\partial y} \\ 0 & \dfrac{\partial}{\partial y} & \dfrac{\partial}{\partial x} \end{bmatrix} \qquad \boldsymbol{\nabla} = \begin{Bmatrix} \dfrac{\partial}{\partial x} \\ \dfrac{\partial}{\partial y} \end{Bmatrix} \tag{2}$$

refer to the orthogonal Cartesian coordinates x and y located in the plate midsurface [31].

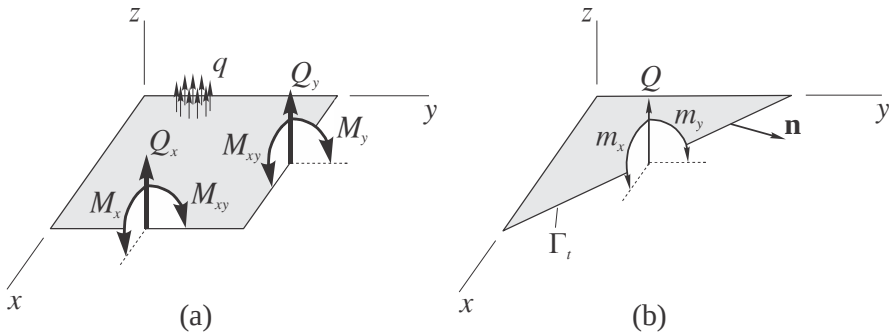

Figure 1: Forces on the plate midsurface: (a) internal forces M_x, M_y, M_{xy}, Q_x and Q_y, and the external distributed transverse load q; (b external forces m_x, m_y and Q acting on Γ_t.

2.2 Mechanical Boundary Conditions

Let Γ be the boundary of the domain Ω, with unit outward normal vector denoted by $\boldsymbol{n} = \lfloor n_x \quad n_y \rfloor^T$. In addition to (1), the moments and shear forces must also satisfy the mechanical boundary conditions

$$\boldsymbol{NM} = \boldsymbol{m} \qquad \boldsymbol{n}^T \boldsymbol{Q} = Q \tag{3}$$

on the portion Γ_t of Γ on which the moments $\boldsymbol{m} = [m_x \quad m_y]^T$ and the shear force Q are prescribed (Figure 1b). Matrix

$$\boldsymbol{N} = \begin{bmatrix} n_x & 0 & n_y \\ 0 & n_y & n_x \end{bmatrix} \tag{4}$$

contains the components of $\boldsymbol{n}$.

2.3 Yield Criteria

The moments and shear forces should satisfy the von Mises yield criterion

$$f(\boldsymbol{M}, \boldsymbol{Q}) \leq 0 \tag{5}$$

written in the moment and shear force space [24-26]. Defining

$$f_M(\boldsymbol{M}) = \frac{M_x^2 + M_y^2 - M_x M_y + 3M_{xy}^2}{M_0^2} \qquad f_Q(\boldsymbol{Q}) = \frac{Q_x^2 + Q_y^2}{Q_0^2} \tag{6}$$

with $M_0 = \sigma_0 h^2/4$ and $Q_0 = \sigma_0 h/\sqrt{3}$ standing for the yield moment and shear force, respectively, the von Mises yield function reads

$$f(\boldsymbol{M}, \boldsymbol{Q}) = f_M(\boldsymbol{M}) + f_Q(\boldsymbol{Q}) - 1. \tag{7}$$

Thus, the yield criterion (5) takes the form

$$\frac{(M_x - M_y)^2 + M_x^2 + M_y^2 + 6M_{xy}^2}{2M_0^2} + \frac{Q_x^2 + Q_y^2}{Q_0^2} \leq 1. \tag{8}$$

The special cases

$$\frac{(M_x - M_y)^2 + M_x^2 + M_y^2 + 6M_{xy}^2}{2M_0^2} \leq 1 \qquad \frac{Q_x^2 + Q_y^2}{Q_0^2} \leq 1 \tag{9}$$

correspond to the infinite shear ($Q_0 \to \infty$) and pure shear ($M_0 \to \infty$) yield criteria, respectively.

3 FINITE ELEMENT FORMULATION

Suppose that the plate is divided into a number of triangular elements and treated as an assembly of them. To apply the equations (1) and (3) to a typical element Ω_e shown in Figure 2, the definition

of the boundary should be extended to include $\mathbf{N}\boldsymbol{M}$ and $\boldsymbol{n}^T\boldsymbol{Q}$ continuity on the interelement portion Γ_i:

$$(\boldsymbol{NM})^+ + (\boldsymbol{NM})^- = \mathbf{0} \qquad (\boldsymbol{n}^T\boldsymbol{Q})^+ + (\boldsymbol{n}^T\boldsymbol{Q})^- = 0 \tag{10}$$

where the superscripts "+" and "−" denote the two sides of Γ_i.

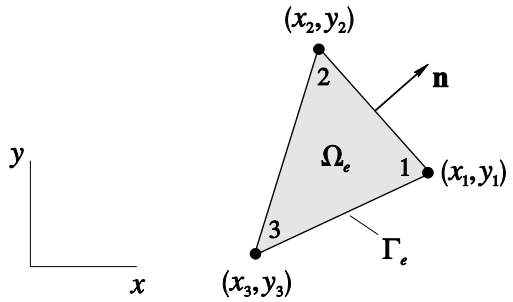

Figure 2: Finite element Ω_e with the unit normal vector $\boldsymbol{n}$ on its boundary Γ_e.

Equations (1), (3) and (10) can be enforced to be satisfied on average over the element and on its boundary by means of

$$\int_{\Omega_e} \left[\boldsymbol{\phi}^T(\boldsymbol{DM} - \boldsymbol{Q}) + w(\boldsymbol{\nabla}^T\boldsymbol{Q} + q)\right] dx\, dy - \int_{\Gamma_t} \left[\boldsymbol{\phi}^T(\boldsymbol{NM} - \boldsymbol{m}) + w(\boldsymbol{n}^T\boldsymbol{Q} - Q)\right] ds$$

$$- \int_{\Gamma_i} \left[\boldsymbol{\phi}^T(\boldsymbol{NM}) + w(\boldsymbol{n}^T\boldsymbol{Q})\right] ds = 0 \tag{11}$$

where $\boldsymbol{\phi} = \begin{bmatrix}\phi_x & \phi_y\end{bmatrix}^T$ and w are arbitrary weight functions that are continuous across the element interfaces. The last integral, when considered jointly with those of the neighborhood elements, enforce (10).

In view of the divergence theorem, we write

$$\int_{\Omega_e} \boldsymbol{\phi}^T(\boldsymbol{DM})\, dx\, dy = \int_{\Gamma_e} \boldsymbol{\phi}^T(\boldsymbol{NM})\, ds - \int_{\Omega_e} (\boldsymbol{D}^T\boldsymbol{\phi})^T\boldsymbol{M}\, dx\, dy$$

$$\int_{\Omega_e} w(\boldsymbol{\nabla}^T\boldsymbol{Q})\, dx\, dy = \int_{\Gamma_e} w(\boldsymbol{n}^T\boldsymbol{Q})\, ds - \int_{\Omega_e} (\boldsymbol{\nabla} w)^T\boldsymbol{Q}\, dx\, dy. \tag{12}$$

Since $\Gamma_e = \Gamma_u \cup \Gamma_t \cup \Gamma_i$, expression (11) is then simplified to

$$\int_{\Gamma_u} \left[\boldsymbol{\phi}^T(\boldsymbol{NM}) + w(\boldsymbol{n}^T\boldsymbol{Q})\right] ds + \int_{\Gamma_t} \left(\boldsymbol{\phi}^T\boldsymbol{m} + wQ\right) ds$$

$$+ \int_{\Omega_e} wq\, dx\, dy - \int_{\Omega_e} \left[(\boldsymbol{D}^T\boldsymbol{\phi})^T\boldsymbol{M} + (\boldsymbol{\nabla}w + \boldsymbol{\phi})^T\boldsymbol{Q}\right] dx\, dy = 0 \tag{13}$$

where the portion Γ_u of the element boundary Γ_e falls on the plate boundary with prescribed displacement.

The moment and shear force fields are linearly approximated over the element by

$$\begin{Bmatrix}\boldsymbol{M}\\ \boldsymbol{Q}\end{Bmatrix} = N_1\begin{Bmatrix}\boldsymbol{M}_1\\ \boldsymbol{Q}_1\end{Bmatrix} + N_2\begin{Bmatrix}\boldsymbol{M}_2\\ \boldsymbol{Q}_2\end{Bmatrix} + N_3\begin{Bmatrix}\boldsymbol{M}_3\\ \boldsymbol{Q}_3\end{Bmatrix} \tag{14}$$

where

$$\boldsymbol{M}_i = \lfloor M_{xi} \quad M_{yi} \quad M_{xyi}\rfloor^T \qquad \boldsymbol{Q}_i = \begin{bmatrix}Q_{xi} & Q_{yi}\end{bmatrix}^T \tag{15}$$

are the moment and shear force nodal values, and

$$N_i = \frac{1}{2A}(\alpha_i + \beta_i x + \gamma_i y) \qquad i = 1,2,3 \tag{16}$$

are the shape functions with A standing for the triangle area. To evaluate

$$\alpha_i = x_j y_k - x_k y_j \qquad \beta_i = y_j - y_k \qquad \gamma_i = x_k - x_j \tag{17}$$

from the node coordinates, the indices i, j and k should be permuted in a natural order ($i \neq j \neq k$). The weight functions are also taken to vary linearly,

$$\begin{Bmatrix}\boldsymbol{\phi}\\ w\end{Bmatrix} = N_1\begin{Bmatrix}\boldsymbol{\phi}_1\\ w_1\end{Bmatrix} + N_2\begin{Bmatrix}\boldsymbol{\phi}_2\\ w_2\end{Bmatrix} + N_3\begin{Bmatrix}\boldsymbol{\phi}_3\\ w_3\end{Bmatrix} \tag{18}$$

with nodal values $\boldsymbol{\phi}_i = \begin{bmatrix}\phi_{xi} & \phi_{yi}\end{bmatrix}^T$ and w_i.

Substitution of (14) and (18) into (13) yields

$$\begin{Bmatrix}\boldsymbol{\phi}_1\\ w_1\\ \boldsymbol{\phi}_2\\ w_2\\ \boldsymbol{\phi}_3\\ w_3\end{Bmatrix}^T \left(\boldsymbol{F} - [\boldsymbol{G}_M \quad \boldsymbol{G}_{Q1} \quad \boldsymbol{G}_M \quad \boldsymbol{G}_{Q2} \quad \boldsymbol{G}_M \quad \boldsymbol{G}_{Q3}]\begin{Bmatrix}\boldsymbol{M}_1\\ \boldsymbol{Q}_1\\ \boldsymbol{M}_2\\ \boldsymbol{Q}_2\\ \boldsymbol{M}_3\\ \boldsymbol{Q}_3\end{Bmatrix}\right) = 0 \tag{19}$$

where

$$\boldsymbol{G}_M = \frac{1}{6}\begin{bmatrix} y_2 - y_3 & 0 & x_3 - x_2 \\ 0 & x_3 - x_2 & y_2 - y_3 \\ 0 & 0 & 0 \\ y_3 - y_1 & 0 & x_1 - x_3 \\ 0 & x_1 - x_3 & y_3 - y_1 \\ 0 & 0 & 0 \\ y_1 - y_2 & 0 & x_2 - x_1 \\ 0 & x_2 - x_1 & y_1 - y_2 \\ 0 & 0 & 0 \end{bmatrix} \qquad \boldsymbol{G}_{Q1} = \frac{1}{6}\begin{bmatrix} A & 0 \\ 0 & A \\ y_2 - y_3 & x_3 - x_2 \\ A/2 & 0 \\ 0 & A/2 \\ y_3 - y_1 & x_1 - x_3 \\ A/2 & 0 \\ 0 & A/2 \\ y_1 - y_2 & x_2 - x_1 \end{bmatrix}$$

$$\boldsymbol{G}_{Q2} = \frac{1}{6}\begin{bmatrix} A/2 & 0 \\ 0 & A/2 \\ y_2 - y_3 & x_3 - x_2 \\ A & 0 \\ 0 & A \\ y_3 - y_1 & x_1 - x_3 \\ A/2 & 0 \\ 0 & A/2 \\ y_1 - y_2 & x_2 - x_1 \end{bmatrix} \qquad \boldsymbol{G}_{Q3} = \frac{1}{6}\begin{bmatrix} A/2 & 0 \\ 0 & A/2 \\ y_2 - y_3 & x_3 - x_2 \\ A/2 & 0 \\ 0 & A/2 \\ y_3 - y_1 & x_1 - x_3 \\ A & 0 \\ 0 & A \\ y_1 - y_2 & x_2 - x_1 \end{bmatrix}$$

$$\boldsymbol{F} = \int_{\Gamma_t} \left(\begin{bmatrix} \boldsymbol{N}_1 \\ \boldsymbol{0} \\ \boldsymbol{N}_2 \\ \boldsymbol{0} \\ \boldsymbol{N}_3 \\ \boldsymbol{0} \end{bmatrix} \boldsymbol{m} + \begin{Bmatrix} 0 \\ N_1 \\ 0 \\ N_2 \\ 0 \\ N_3 \end{Bmatrix} Q \right) ds + \int_{\Omega_e} \begin{Bmatrix} 0 \\ N_1 \\ 0 \\ N_2 \\ 0 \\ N_3 \end{Bmatrix} q \, dx \, dy \tag{20}$$

and

$$\boldsymbol{N}_i = \begin{bmatrix} N_i & 0 \\ 0 & N_i \end{bmatrix} \qquad \boldsymbol{0} = \lfloor 0 \quad 0 \rfloor. \tag{21}$$

Because (19) holds for any arbitrary weight functions, it follows that

$$[\boldsymbol{G}_M \quad \boldsymbol{G}_{Q1} \quad \boldsymbol{G}_M \quad \boldsymbol{G}_{Q2} \quad \boldsymbol{G}_M \quad \boldsymbol{G}_{Q3}] \begin{Bmatrix} \boldsymbol{M}_1 \\ \boldsymbol{Q}_1 \\ \boldsymbol{M}_2 \\ \boldsymbol{Q}_2 \\ \boldsymbol{M}_3 \\ \boldsymbol{Q}_3 \end{Bmatrix} = \boldsymbol{F}. \tag{22}$$

Elimination of the integral over Γ_u by choosing $\boldsymbol{\phi}$ and w null over there introduces zero components of $\boldsymbol{\phi}_i$ or w_i into (19) which must be accounted for in (22) by removing the respective equations. Thus, the element enforces the equilibrium equations (1) and the mechanical boundary conditions (3) to be satisfied by the discrete equation (22) on average accordingly to (13). The element development has its roots in the classic paper by Anderheggen and Knöpfel [27].

4 PLASTIC ADMISSIBILITY

It can be shown that the yield criterion (8) is satisfied throughout the proposed element as long as it is satisfied at the element nodes. Thus, the imposition of the criterion at the three nodes,

$$\begin{aligned}
&\frac{\left(M_{x1}-M_{y1}\right)^2+M_{x1}^2+M_{y1}^2+6M_{xy1}^2}{2M_0^2}+\frac{Q_{x1}^2+Q_{y1}^2}{Q_0^2}\le 1\\
&\frac{\left(M_{x2}-M_{y2}\right)^2+M_{x2}^2+M_{y2}^2+6M_{xy2}^2}{2M_0^2}+\frac{Q_{x2}^2+Q_{y2}^2}{Q_0^2}\le 1\\
&\frac{\left(M_{x3}-M_{y3}\right)^2+M_{x3}^2+M_{y3}^2+6M_{xy3}^2}{2M_0^2}+\frac{Q_{x3}^2+Q_{y3}^2}{Q_0^2}\le 1,
\end{aligned} \tag{23}$$

implies the satisfaction of

$$\frac{\left(M_x-M_y\right)^2+M_x^2+M_y^2+6M_{xy}^2}{2M_0^2}+\frac{Q_x^2+Q_y^2}{Q_0^2}\le 1 \tag{24}$$

throughout the element. To prove what has been asserted, we introduce the linear interpolation (14) into the left-hand side of (24) to obtain

$$LHS = k_1N_1^2+k_2N_2^2+k_3N_3^2+2k_{12}N_1N_2+2k_{13}N_1N_3+2k_{23}N_2N_3 \tag{25}$$

where

$$\begin{aligned}
k_i &= \frac{\left(M_{xi}-M_{yi}\right)^2+M_{xi}^2+M_{yi}^2+6M_{xyi}^2}{2M_0^2}+\frac{Q_{xi}^2+Q_{yi}^2}{Q_0^2}\\
k_{ij} &= \frac{\left(M_{xi}-M_{yi}\right)\left(M_{xj}-M_{yj}\right)+M_{xi}M_{xj}+M_{yi}M_{yj}+6M_{xyi}M_{xyj}}{2M_0^2}+\frac{Q_{xi}Q_{xj}+Q_{yi}Q_{yj}}{Q_0^2}\\
&\qquad\qquad i,j=1,2,3
\end{aligned} \tag{26}$$

From (23), it is apparent that $k_i \le 1$. Adding the first two inequalities (23),

$$\frac{\left[\left(M_{x1}-M_{y1}\right)^2+\left(M_{x2}-M_{y2}\right)^2\right]+\left(M_{x1}^2+M_{x2}^2\right)+\left(M_{y1}^2+M_{y2}^2\right)+6\left(M_{xy1}^2+M_{xy2}^2\right)}{2M_0^2}$$

$$+\frac{\left(Q_{x1}^2+Q_{x2}^2\right)+\left(Q_{y1}^2+Q_{y2}^2\right)}{Q_0^2}\leq 2, \tag{27}$$

and knowing that $2ab \leq a^2 + b^2$ is true for any number a, b and c, inequality (27) implies

$$\frac{\left[2\left(M_{x1}-M_{y1}\right)\left(M_{x2}-M_{y2}\right)\right]+\left(2M_{x1}M_{x2}\right)+\left(2M_{y1}M_{y2}\right)+6\left(2M_{xy1}M_{xy2}\right)}{2M_0^2}$$

$$+\frac{\left(2Q_{x1}Q_{x2}\right)+\left(2Q_{y1}Q_{y2}\right)}{Q_0^2}\leq 2. \tag{28}$$

This result shows that $k_{12} \leq 1$. The two other similar combinations of inequalities (23) will give k_{13}, $k_{23} \leq 1$. Since all the coefficients k_i, k_{ij} in (25) are bounded by 1 and $N_1 + N_2 + N_3 = 1$, we finally write

$$LHS \leq (N_1 + N_2 + N_3)^2 = 1. \tag{29}$$

Therefore, satisfying the yield criterion (8) at the element nodes implies satisfying it throughout the element.

5 THE SOCP PROBLEM

In the lower bound limit analysis, the equilibrium equations, the mechanical boundary conditions and the yield criterion, expressed in terms of nodal moments and shear forces, are constraints of an optimization problem for the applied load maximization. The optimal solution

$$\lambda^* = \{\max \lambda \mid \boldsymbol{l}\bar{\boldsymbol{\sigma}} = \lambda \boldsymbol{f}_1 + \boldsymbol{f}_2,\ \boldsymbol{g}(\bar{\boldsymbol{\sigma}}) \leq \boldsymbol{0}\} \tag{30}$$

identifies the collapse load, where the applied load has been splitted into two parts: $\lambda \boldsymbol{f}_1$ which is adjusted during the optimization by means of the load factor λ, and $\boldsymbol{f}_2$ which is kept constant. Vector $\bar{\boldsymbol{\sigma}}$ collects the nodal moments and shear forces.

The equality constraint

$$\boldsymbol{l}\bar{\boldsymbol{\sigma}} = \lambda \boldsymbol{f}_1 + \boldsymbol{f}_2 \tag{31}$$

arises from the assembly of (22). The inequality constraint

$$\boldsymbol{g}(\bar{\boldsymbol{\sigma}}) \leq \boldsymbol{0} \tag{32}$$

stems from the evaluation at each mesh node of inequality (8).

The nonlinear convex optimization problem (30) is not a SOCP problem. To formulate it as such [28], we introduce the auxiliary variables

$$\boldsymbol{v} = \begin{Bmatrix} v_1 \\ v_2 \\ v_3 \\ v_4 \\ v_5 \\ v_6 \end{Bmatrix} = \begin{bmatrix} \frac{1}{\sqrt{2}\mathrm{M}_0} & -\frac{1}{\sqrt{2}\mathrm{M}_0} & 0 & 0 & 0 & 0 \\ \frac{1}{\sqrt{2}\mathrm{M}_0} & 0 & 0 & 0 & 0 & 0 \\ 0 & \frac{1}{\sqrt{2}\mathrm{M}_0} & 0 & 0 & 0 & 0 \\ 0 & 0 & \frac{\sqrt{3}}{\mathrm{M}_0} & 0 & 0 & 0 \\ 0 & 0 & 0 & \frac{1}{\mathrm{Q}_0} & 0 & 0 \\ 0 & 0 & 0 & 0 & \frac{1}{\mathrm{Q}_0} & 0 \end{bmatrix} \begin{Bmatrix} M_x \\ M_y \\ M_{xy} \\ Q_x \\ Q_y \end{Bmatrix} \tag{33}$$

into (8) to state $f(\boldsymbol{M}, \boldsymbol{Q}) \leq 0$ as the six-dimensional second-order cone

$$\sqrt{v_1^2 + v_2^2 + v_3^2 + v_4^2 + v_5^2 + v_6^2} \leq 1. \tag{34}$$

Now, the problem can be treated as SOCP by just replacing $\boldsymbol{g}(\bar{\boldsymbol{\sigma}}) \leq \mathbf{0}$ with

$$\boldsymbol{h}_1(\bar{\boldsymbol{\sigma}}, \bar{\boldsymbol{v}}) = \mathbf{0} \qquad \boldsymbol{h}_2(\bar{\boldsymbol{v}}) \leq \mathbf{0} \tag{35}$$

where the vector $\bar{\boldsymbol{v}}$ collects the nodal values of $\boldsymbol{v}$. The new constraints (35) stem from the evaluation of (33) and (34) at each node.

For the special cases of infinite shear and pure shear yield criteria (9), the second-order cone reduces to four and two dimensions, respectively.

The optimization problem solution is carried out following the step: (a) set up of the SOCP problem with YALMIP [32] in the MATLAB environment: problem (30) with (32) replaced by (35); (b) solution by MOSEK [33] which contains a robust interior-point optimizer for nonlinear convex optimization developed by Andersen *et al.* [13].

6 NUMERICAL EXAMPLES

To assess the accuracy of the finite element proposed for lower bound limit analysis of Reissner-Mindlin plates two benchmark examples are tested. The results are compared to exact solutions and/or numerical lower/upper bounds available in the literature. The computations are

performed on a Sony VAIO™ All-in-One machine (i5 dual core 2.50 GHz CPU, 12 GB RAM) running a 64-bit Windows 7.

6.1 Square Plates

First it is analyzed the problem of a square plate of side length $L = 1\ m$ subjected to a uniform out-of-plane distributed load q with two different edge 'hard' boundary conditions: simple supports or clamped supports on all edges. Because we have two axes of symmetry, we consider only the bottom left quarter of the plate in the analysis (Figure 3).

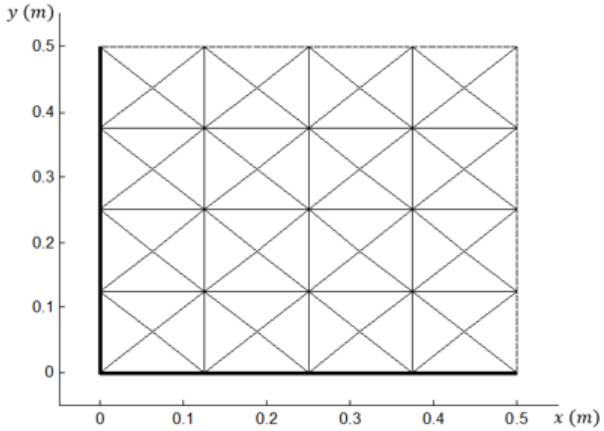

Figure 3: Square plate adopted domain: structured 4×4 mesh.

The mechanical boundary conditions at the upper and right symmetry edges are $M_{ns} = Q_n = 0$. As M_n is unknown at the symmetry edges, the weight function component φ_n should be set equal to zero at nodes belonging to these edges. For the bottom and left plate edges, simple supports ($M_n = \varphi_s = w = 0$) and clamped supports ($\varphi_n = \varphi_s = w = 0$) are investigated. The slenderness ratio of the plate is defined as $\delta = L/h$. Five different structured meshes are examined, where the number of elements E and the number of stress variables NSV for each mesh is detailed in Table 1.

Table 1: Square plate meshes and the respective number of elements and stress variables.

$n \times n$	E	NSV
4×4	64	123
8×8	256	435
16×16	1024	1635
32×32	4096	6339
64×64	16384	24963

6.1.1 Thin 'Square Plate' Solution with the Infinite Shear Yield Criterion

It is adopted first the infinite shear yield criterion. It can be easily seen that the collapse load is proportional to M_0/L^2 [34], meaning the lower bound load factor can be written as $q\,L^2/M_0$.

Table 2 condenses the lower bounds obtained with the five different meshes and the difference to Kirchhoff upper bound references found in: Le *et al.* [20] for the clamped plate; and Bleyer and de Buhan [25] for the simply supported plate. As expected, the results are independent of the slenderness ratio and this was verified by achieving the same values for ten different slenderness ratios (δ = 1, 2, 4, 8, 10, 20, 40, 80, 100, 200). Our estimates for the simply supported plate with 8×8, 16×16, 32×32 and 64×64 meshes are less than 1% distant from Bleyer and de Buhan upper bound. Our prediction for the clamped plate with 64×64 mesh is less than 1% distant from Le *et al.* upper bound. For the simply supported case, the proposed scheme converges to the Kirchhoff thin plate upper bound reference from under it. For the clamped case, it converges to the Kirchhoff thin plate upper bound reference from above it. In the following, our lower bound estimates obtained with a very refined mesh (64×64) will serve as reference values of thin plate solutions and will be noted $q(\delta = \infty)$.

Table 2: Comparison of the lower bounds computed with the infinite shear yield criterion ($Q_0 \to \infty$) to Kirchhoff (thin) plate upper bound estimates found in [20] and [25].

n	Simply supported qL^2/M_0	Clamped qL^2/M_0
4	24.0109 (−4.08%)†	71.9416 (59.44%)†
8	24.9673 (−0.26%)	56.0464 (24.22%)
16	25.0031 (−0.12%)	49.6602 (10.06%)
32	25.0145 (−0.074%)	46.7726 (3.66%)
64	25.0177 (−0.06%)	45.4029 (0.63%)
Upper bound	25.033	45.12

†relative difference in percentage when compared to the respective Kirchhoff upper bound reference.

6.1.2 Influence of the Slenderness Ratio on the Lower Bound of 'Square Plates'

The influence of the slenderness ratios on the lower bound is studied with 8×8, 16×16 and 32×32 meshes. Table 3 illustrates our predictions for various slenderness ratios considering the von Mises yield criterion (finite M_0 and Q_0). The results for the simply supported condition, with all three meshes, converge monotonically to the thin plate reference solution as the slenderness ratio increases. The results for the clamped condition converge monotonically to the thin plate reference solution as the slenderness ratio increases only with 32×32 mesh.

Table 3: Clamped and simply supported square plates with the von Mises yield criterion: normalized results for different slenderness ratios.

δ	Simply supported†			Clamped‡		
	8×8	16×16	32×32	8×8	16×16	32×32
	$q/q(\delta = \infty)$	$q/q(\delta = \infty)$	$q/q(\delta = \infty)$	$q/q(\delta = \infty)$	$q/q(\delta = \infty)$	$q/q(\delta = \infty)$
1	0.3622	0.3546	0.3511	0.1998	0.1955	0.1935
2	0.6971	0.6929	0.6901	0.3958	0.3896	0.3862
4	0.9323	0.9343	0.9348	0.6635	0.6549	0.6497
8	0.9785	0.9806	0.9811	0.8713	0.8592	0.8526
10	0.9849	0.9870	0.9876	0.9128	0.8990	0.8920
20	0.9941	0.9961	0.9967	0.9864	0.9647	0.9549
40	0.9966	0.9985	0.9991	1.0230	0.9888	0.9750
80	0.9974	0.9991	0.9997	1.0680	1.0023	0.9830
100	0.9975	0.9992	0.9997	1.0901	1.0068	0.9848
200	0.9978	0.9993	0.9998	1.1872	1.0276	0.9897

†results normalized by the simply supported thin plate reference solution $q(\delta = \infty) = 25.0177\, M_0/L^2$.
‡results normalized by the clamped thin plate reference solution $q(\delta = \infty) = 45.4029\, M_0/L^2$.

It is also investigated, based on 32×32 mesh, the evolution of our lower bounds with respect to δ considering the pure shear yield criterion ($M_0 \to \infty$). Results for both yield criteria and both support conditions are presented in Table 4 and plotted in Figure 4 (simply supported) and in Figure 5 (clamped). Table 4 demonstrate that in the case of a plate subjected to the pure shear yield criterion the critical load is independent from the boundary conditions, which is in accordance with what is stated in [24, 25]. The same argumentation is valid in the thick plate limit ($\delta = 1$) for the von Mises yield criterion.

Table 4: Clamped and simply supported square plates based on 32×32 mesh and different yield criteria: results for different slenderness ratios.

δ	Simply supported		Clamped	
	$M_0 \to \infty$	$Finite\ M_0\ and\ Q_0$	$M_0 \to \infty$	$Finite\ M_0\ and\ Q_0$
	qL^2/M_0	qL^2/M_0	qL^2/M_0	qL^2/M_0
1	8.7867	8.7843	8.7867	8.7858
2	17.5734	17.2653	17.5734	17.5339
4	35.1468	23.3872	35.1468	29.4989
8	70.2937	24.5460	70.2937	38.7083
10	87.8671	24.7064	87.8671	40.4998
20	175.7343	24.9342	175.7343	43.3536
40	351.4686	24.9940	351.4686	44.2672
80	702.9372	25.0093	702.9372	44.6327
100	878.6707	25.0111	878.6707	44.7116
200	1,757.3414	25.0136	1,757.3414	44.9366

Figures 4 and 5 indicate that for $\delta \geq 8$ (and $\delta \geq 80$ for the clamped case) the computed lower bounds are close to the thin plate solution (by less than 2%), i.e., solutions obtained using Reissner-Mindlin model converge to Kirchhoff's when $\delta \to \infty$. Furthermore, as again expected, for thick plates with $1 \leq \delta \leq 2$, the shear forces command the collapse, while for plates with $\delta \geq 8$ (and $\delta \geq 80$ for the clamped case) the moments rule the collapse behavior. Thus, a simply supported plate with $\delta \geq 8$ can be considered thin enough to eliminate the effects of transverse shear strains; the same

argumentation holds for a clamped plate with $\delta \geq 80$. It must also be noted that plates having clamped boundary conditions converge slower than those with simply supported boundaries.

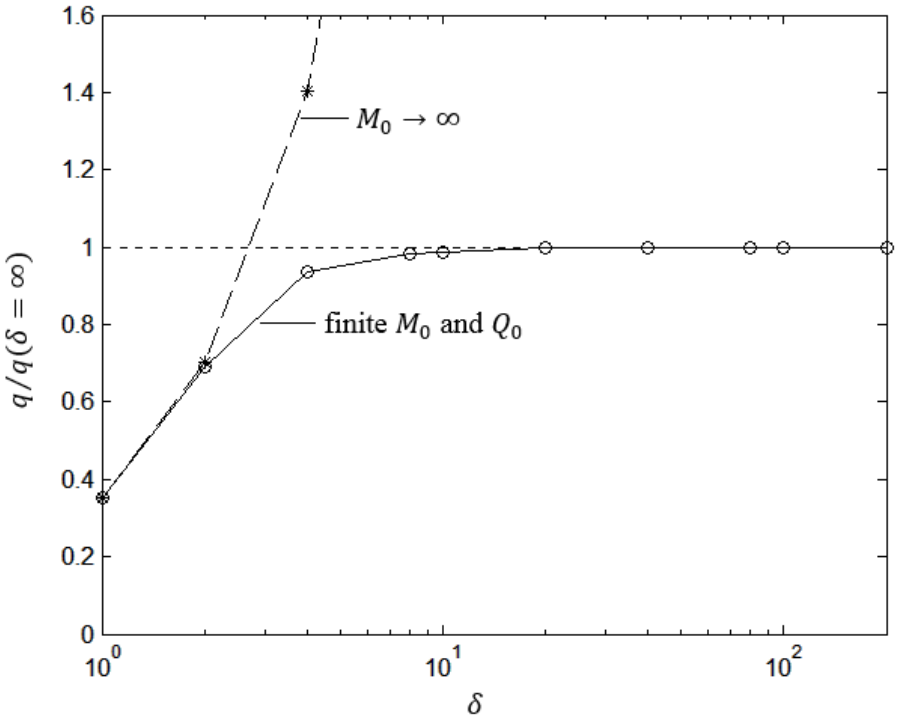

Figure 4: Evolution of the lower bound estimate for simply supported square plates, based on 32×32 mesh, with respect to the slenderness ratio δ. Results normalized by the thin plate reference solution $q(\delta = \infty) = 25.0177\, M_0/L^2$.

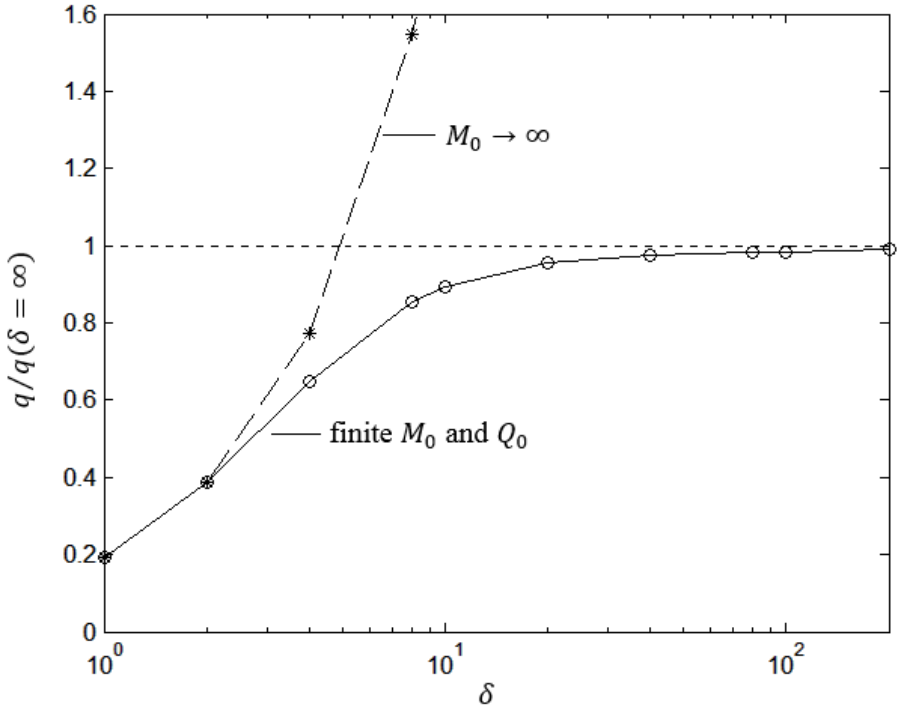

Figure 5: Evolution of the lower bound estimate for clamped square plates, based on 32×32 mesh, with respect to the slenderness ratio δ. Results normalized by the thin plate reference solution $q(\delta = \infty) = 45.4029\, M_0/L^2$.

6.2 Circular Plates

In this example, lower bounds of hard simply supported ($M_n = \varphi_s = w = 0$) and clamped ($\varphi_n = \varphi_s = w = 0$) circular plates of radius $R = 1\, m$ are computed when subjected to either a uniformly distributed or a concentrated central load, denoted as q and P, respectively (Figure 6). Owing to the symmetry conditions, only one quadrant of the domain was modelled, using five different structured meshes (6×6 mesh depicted in Figure 6). The mechanical boundary conditions at the bottom and left symmetry edges are $M_{ns} = Q_n = 0$. As M_n is unknown at the symmetry edges, the weight function component φ_n should be set equal to zero. The number of elements and the number of stress variables for each mesh is detailed in Table 5.

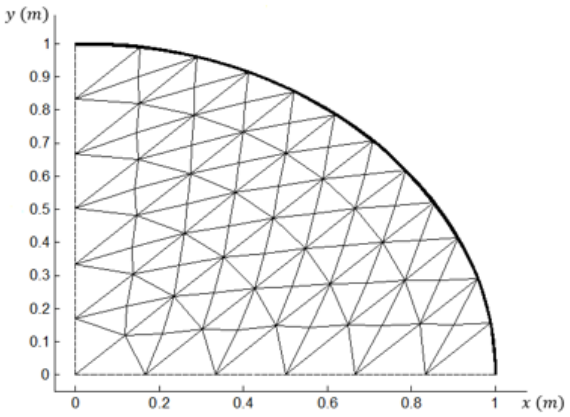

Figure 6: Circular plate adopted domain: structured 6×6 mesh.

Table 5: Circular plate meshes and the respective number of elements and stress variables.

$n \times n$	E	NSV
3×3	30	66
6×6	132	237
12×12	552	903
24×24	2256	3531
48×48	9120	13971

For the uniformly distributed load the lower bound load factor can be written as $q\,R^2/M_0$. For the central concentrated load $\lambda = P/M_0$. The computed lower bounds are given in terms of its respective load factor. Our predictions with the von Mises yield criterion (finite M_0 and Q_0) under uniformly distributed load for both edge boundary conditions and various slenderness ratios $\delta = R/h$ are presented in Tables 6 and 7. As it can be seen, the proposed scheme demonstrate excellent performance, especially with the most refined mesh, revealing a convergence of results to the Kirchhoff (thin) solutions as the plate thickness is reduced.

Table 6: Simply supported circular plates under uniformly distributed load with the von Mises yield criterion: results for different slenderness ratios and meshes.

δ	3×3	6×6	12×12	24×24	48×48
	qR^2/M_0	qR^2/M_0	qR^2/M_0	qR^2/M_0	qR^2/M_0
1	4.7629	4.7606	4.7093	4.6623	4.6393
2	6.0047	5.9959	5.9977	5.9985	5.9987
4	6.4406	6.3822	6.3783	6.3784	6.3785
8	6.6654	6.4979	6.4822	6.4813	6.4813
10	6.7394	6.5176	6.4955	6.4939	6.4939
20	7.0338	6.5739	6.5162	6.5111	6.5108
40	7.4956	6.6600	6.5302	6.5163	6.5151
80	8.3183	6.8109	6.5519	6.5198	6.5164
100	8.7180	6.8786	6.5623	6.5212	6.5165
Collapse load[†]			6.52		

[†] collapse load obtained by Hopkins and Wang [35] using Kirchhoff (thin) plate assumptions.

Table 7: Clamped circular plates under uniformly distributed load with the von Mises yield criterion: results for different slenderness ratios and meshes.

δ	3×3	6×6	12×12	24×24	48×48
	qR^2/M_0	qR^2/M_0	qR^2/M_0	qR^2/M_0	qR^2/M_0
1	5.0541	4.8285	4.7141	4.6630	4.6394
2	8.5735	8.5042	8.4294	8.3628	8.3238
4	11.7173	11.4409	11.2681	11.1535	11.0898
8	13.8845	12.8243	12.4488	12.2838	12.2028
10	14.5156	13.0717	12.6218	12.4406	12.3557
20	17.0870	13.6845	12.9156	12.6685	12.5692
40	21.0657	14.5325	13.1127	12.7532	12.6300
80	27.1688	15.8346	13.4018	12.8234	12.6563
100	30.0804	16.3251	13.5167	12.8524	12.6638
Collapse load†			12.5		

†collapse load obtained by Hopkins and Wang [35] using Kirchhoff (thin) plate assumptions.

The estimates computed considering the von Mises yield criterion, central concentrated load, 48×48 mesh and a thin plate with $\delta = 100$ are: $P = 6.1676M_0$ for simple supports (error of -1.84% when compared to the ultimate load of $2\pi M_0$ obtained using Kirchhoff plate assumptions); and $P = 7.2270M_0$ for clamped supports (error of -0.39% when compared to the ultimate load of $4\pi M_0/\sqrt{3}$ obtained using Kirchhoff plate assumptions). These exact thin plate solutions are available in [36]. The usage of a more refined mesh around the point of loading should provide better lower bound estimates.

In the thick plate limit with $\delta = 0.5$, a lower bound of $q = 2.3197\, M_0/L^2$ is obtained with the von Mises and the pure shear yield criteria for both boundary conditions and under uniformly distributed load. This result is in close agreement to the exact solution considering the pure shear yield criterion:

$$\frac{q_{\text{exact}}L^2}{M_0} = \frac{4}{\sqrt{3}}\frac{2R}{h} = 2.309 \tag{36}$$

with $R/h = 0.5$. This solution is independent of the edge boundary conditions.

Figures 7 and 8 depicts the results of Tables 6 and 7, respectively, based on the finest mesh together with the above-cited thin plate reference collapse loads and the upper bounds found in Capsoni and Vicente da Silva [21] and based on their finest mesh with the $N4\bar{B}0$ element and soft boundary conditions assumptions.

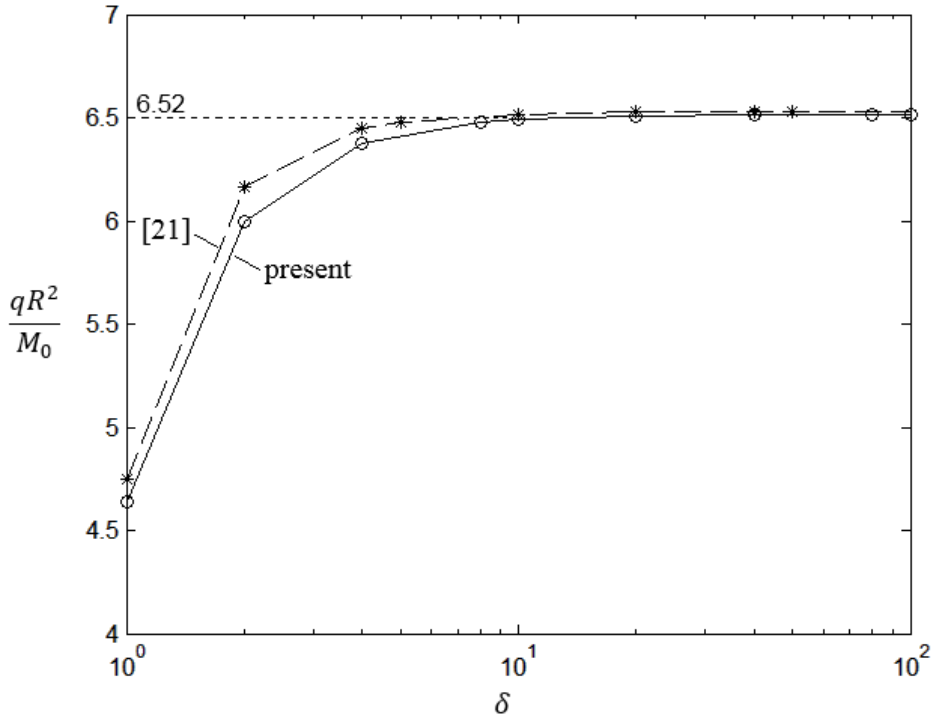

Figure 7: Evolution of the lower bound estimate for simply supported circular plates with respect to the slenderness ratio δ for 32×32 mesh and the von Mises yield criterion.

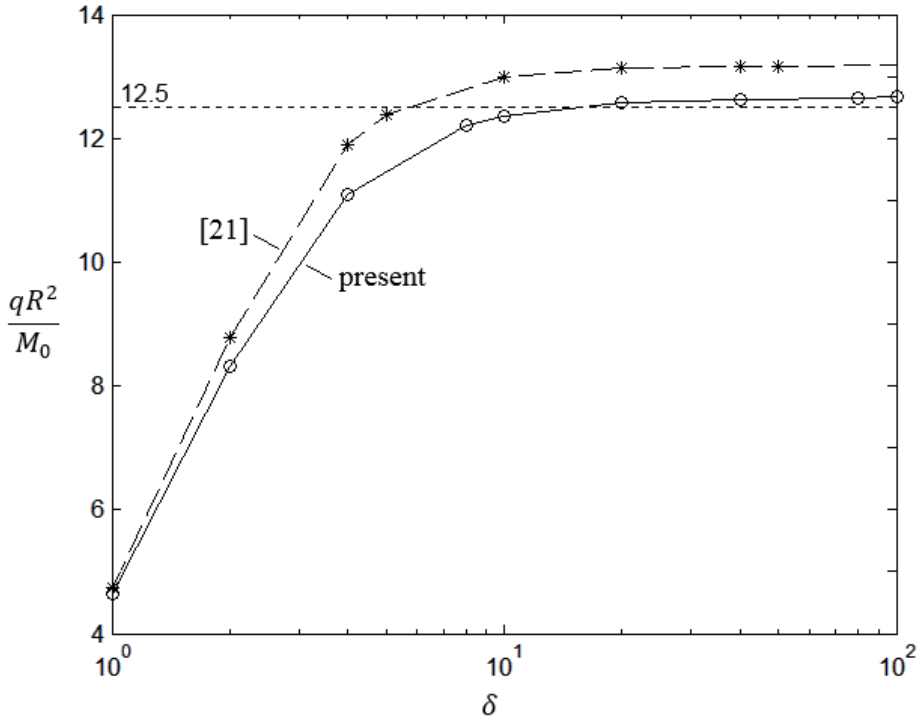

Figure 8: Evolution of the lower bound estimate for clamped circular plates with respect to the slenderness ratio δ for 32×32 mesh and the von Mises yield criterion.

7 CONCLUSION

The paper proposes a numerical approach for computing static limit loads of Reissner-Mindlin plates by combining discretization into simple triangular elements and second-order cone programming. Examples illustrate that the above scheme provides excellent results and the fact of not satisfying the equilibrium equations and the mechanical boundary conditions rigorously is far from being a severe handicap for the developed element. The convergence may not be monotonic, or even from below, but very accurate results are soon reached.

REFERENCES

[1] D.C. Drucker, W. Prager, H.J. Greenberg, (1952), 'Extended limit design theorems for continuous media', Quarterly Journal of Applied Mathematics, 9 (4), 381-389.

[2] D.J. Hayes, P.V. Marçal, (1967), 'Determination of upper bounds for problems in plane stress using finite element techniques', International Journal of Mechanical Sciences, 9 (5), 245-251.

[3] P.G. Hodge, T. Belytschko, (1968), 'Numerical methods for the limit analysis of plates', Journal of Applied Mechanics, 35(4), 796-802.

[4] J. Lysmer, (1970), 'Limit analysis of plane problems in soil mechanics', Journal of the Soil Mechanics and Foundations Division, 96(SM4), 1311-1334.

[5] S.W. Sloan, (1988), 'A steepest edge active set algorithm for solving sparse linear programming problems', International Journal of Numerical Methods in Engineering, 26(12), 2671-2685.

[6] E. Christiansen, K.O. Kortanek, (1991), 'Computation of the collapse state in limit analysis using the LP primal affine scaling algorithm', Journal of Computational and Applied Mathematics, 34(1), 47-63.

[7] N. Zouain, J. Herskovits, L.A. Borges, R.A. Feijóo, (1993), 'An iterative algorithm for limit analysis with nonlinear yield functions', International Journal of Solids and Structures, 30(10), 1397-1417.

[8] K.D. Andersen, E. Christiansen, (1995), 'Limit analysis with the dual affine scaling algorithm', Journal of Computational and Applied Mathematics, 59(2), 233-243.

[9] K.D. Andersen, (1996), 'A modified Schur-complement method for handling dense columns in interior-point methods for linear programming', ACM Transactions on Mathematical Software, 22(3), 348-356.

[10] Y.E. Nesterov, M.J. Todd, (1998), 'Primal-dual interior-point methods for self-scaled cones', SIAM Journal on Optimization, 8(2), 324-364.

[11] J.F. Sturm, (1999), 'Using SeDuMi 1.02, a MATLAB toolbox for optimization over symmetric cones', Optimization Methods and Software, 11-12, 625-653.

[12] K.D. Andersen, E. Christiansen, A.R. Conn, M.L. Overton, (2000), 'An efficient primal-dual interior-point method for minimizing a sum of Euclidean norms', SIAM Journal on Scientific Computing, 22(1), 243-262.

[13] E.D. Andersen, C. Roos, T. Terlaky, (2003), 'On implementing a primal-dual interior-point method for conic quadratic optimization', Mathematical programming, Series B, 95(2), 249-277.

[14] R.H. Tütüncü, K.C. Toh, M.J. Todd (2003), 'Solving semidefinite-quadratic-linear programs using SDPT3', Mathematical Programming, Series B, 95, 189-217.

[15] J.C. Nagtegaal, D.M. Parks, J.R. Rice. On numerically accurate finite element solutions in the fully plastic range. Computer Methods in Applied Mechanics and Engineering, 4(2), 153-177 (1974).

[16] A. Cecchi, G Milani, A. Tralli, (2007), 'A Reissner-Mindlin limit analysis model for out-of-plane loaded running bond masonry walls', International Journal of Solids and Structures, 44(5), 1438-1460.

[17] C.V. Le, M. Gilbert, H. Askes, (2009), 'Limit analysis of plates using the EFG method and second-order cone programming', International Journal for Numerical Methods in Engineering, 78(13), 1532-1552.

[18] C.V. Le, H. Nguyen-Xuan, H. Askes, S.P.A. Bordas, T. Rabczuk, H. Nguyen-Vinh, (2010), 'A cell-based smoothed finite element method for kinematic limit analysis', International Journal for Numerical Methods in Engineering, 83(12), 1651-1674.

[19] C.V. Le, H. Askes, M. Gilbert, (2010), 'Adaptive element-free Galerkin method applied to the limit analysis of plates', Computer Methods in Applied Mechanics and Engineering, 199(37-40), 2487-2496.

[20] C.V. Le, H. Nguyen-Xuan, H. Nguyen-Dang, (2010), 'Upper and lower bound limit analysis of plates using FEM and second-order cone programming'. Computers & Structures, 88(1-2), 65-73.

[21] A. Capsoni, M. Vicente da Silva, (2011), 'A finite element formulation of Mindlin plates for limit analysis', International Journal for Numerical Methods in Biomedical Engineering, 27(1), 143-156.

[22] H. Nguyen-Xuan, T. Rabczuk, T. Nguyen-Thoi, T.N. Tran, N. Nguyen-Thanh, (2012), 'Computation of limit and shakedown loads using a node-based smoothed finite element method', International Journal for Numerical Methods in Engineering, 90(3), 287-310.

[23] J. Bleyer, P. de Buhan, (2013), 'On the performance of non-conforming finite elements for the upper bound limit analysis of plates', International Journal for Numerical Methods in Engineering, 94(3), 308-330.

[24] C.V. Le, (2013), 'A stabilized discrete shear gap finite element for adaptive limit analysis of Mindlin-Reissner plates'. 'International Journal for Numerical Methods in Engineering', 96(4), 231-246.

[25] J. Bleyer, P. de Buhan, (2014), 'Lower bound static approach for the yield design of thick plates', International Journal for Numerical Methods in Engineering, 100(11), 814-833.

[26] T. Nguyen-Thoi, P. Phung-Van, M.H. Nguyen-Thoi, H. Dang-Trung, (2015), 'An upper-bound limit analysis of Mindlin plates using CS-DSG3 method and second-order cone programming', Journal of Computational and Applied Mathematics, 281, 32-48.

[27] E. Anderheggen, H. Knöpfel, (1972), 'Finite element limit analysis using linear programming', International Journal of Solids and Structures, 8(12), 1413-1431.

[28] M.S. Lobo, L. Vandenberghe, S. Boyd, H. Lebret, (1998), 'Applications of second-order cone programming', Linear Algebra and its Applications, 284(1-3), 193-228.

[29] S. Boyd, L. Vandenberghe, (2009), Convex Optimization, Cambridge University Press, Cambridge.

[30] W.F. Chen, (1975), Limit Analysis and Soil Plasticity, Elsevier, Amsterdam.

[31] J.N. Reddy, (2007), Theory and Analysis of Elastic Plates and Shells, 2nd edition, CRC Press, Boca Raton.

[32] J. Löfberg, (2004), 'YALMIP: A toolbox for modeling and optimization in MATLAB', In Proceedings of the IEEE CSS International Symposium on Computer Aided Control System Design, 284-289, Taipei.

[33] MOSEK ApS, (2016), 'Modeling cookbook'. Available from https://mosek.com/resources/doc/.

[34] J. Lubliner, (2006), Plasticity Theory, revised edition in PDF, previously published by Pearson Education Inc.

[35] H.G. Hopkins, A.J. Wang, (1955), 'Load-carrying capacities for circular plates of perfectly-plastic material with arbitrary yield condition', Journal of the Mechanics and Physics of Solids, 3(2), 117-129.

[36] M. Save, C. Massonnet, G. de Saxce, (1997), Plastic Limit Analysis of Plates, Shells, and Disks. North Holland Series in Applied Mathematics and Mechanics, vol. 43.

RESPONSIBILITY NOTICE

The authors are the only responsible for the printed material included in this paper.